The Journal of Immunology

The Attachment (G) Glycoprotein of Respiratory Syncytial Virus Contains a Single Immunodominant Epitope That Elicits Both Th1 and Th2 CD4$^+$ T Cell Responses

Steven M. Varga, Erika L. Wissinger and Thomas J. Braciale

J Immunol 2000; 165:6487-6495; ;
doi: 10.4049/jimmunol.165.11.6487
http://www.jimmunol.org/content/165/11/6487

The Journal of Immunology is published twice each month by
The American Association of Immunologists, Inc.,
1451 Rockville Pike, Suite 650, Rockville, MD 20852

Print ISSN: 0022-1767 Online ISSN: 1550-6606.

The Attachment (G) Glycoprotein of Respiratory Syncytial Virus Contains a Single Immunodominant Epitope That Elicits Both Th1 and Th2 CD4$^+$ T Cell Responses[1]

Steven M. Varga,* Erika L. Wissinger,† and Thomas J. Braciale[2]*†

BALB/c mice immunized with a vaccinia virus expressing the attachment (G) glycoprotein of respiratory syncytial virus (RSV) develop a virus-specific CD4$^+$ T cell response that consists of a mixture of Th1 and Th2 CD4$^+$ T cells following intranasal infection with live RSV. Recent work has shown that both Th1 and Th2 CD4$^+$ T cells are elicited to a single region comprising aa 183–197 of the G protein. To more precisely define the CD4$^+$ T cell epitope(s) contained within this region, we created a panel of amino- and carboxyl-terminal truncated as well as single alanine-substituted peptides spanning aa 183–197. These peptides were used to examine the ex vivo cytokine response of memory effector CD4$^+$ T cells infiltrating the lungs of G-primed RSV-infected mice. Analysis of lung-derived memory effector CD4$^+$ T cells using intracellular cytokine staining and/or ELISA of effector T cell culture supernatants revealed a single I-E^d-restricted CD4$^+$ T cell epitope with a core sequence mapping to aa 185–193. In addition, we examined the T cell repertoire of the RSV G peptide-specific CD4$^+$ T cells and show that the CD4$^+$ T cells directed to this single immunodominant G epitope use a restricted range of TCR Vβ genes and predominantly express Vβ14 TCR. ***The Journal of Immunology,*** **2000, 165: 6487–6495.**

CD4$^+$ T cells play a central role in regulating humoral and cellular immune responses. During virus infections, CD4$^+$ T cells can provide help to B cells in the production of neutralizing Abs, can provide help for the generation of cytotoxic CD8$^+$ T cell responses, and can act as effector cells themselves as a consequence of the wide range of cytokines that they can produce (1–3). Despite the important role CD4$^+$ T cells play in regulating immune responses, surprisingly little information is known about the specificity and frequency of these cells during virus infections.

Respiratory syncytial virus (RSV)[3] is a ubiquitous human respiratory pathogen. Clinically apparent infection most frequently occurs in young children. It is estimated that 60% of infants are infected within their first year of life (4). RSV is the leading cause of viral lower respiratory tract infection worldwide, accounting for >90,000 hospitalizations in the United States each year (5). In addition to children, RSV infection is also an important cause of severe respiratory illness in elderly and immunocompromised individuals (6–10). Despite the significant health and economic burden produced by RSV, currently there is no safe and effective licensed RSV vaccine. Early RSV vaccine trials in human children using formalin-inactivated (FI)-RSV had to be halted because children receiving the FI-RSV vaccine displayed greater morbidity and mortality with subsequent natural RSV infection than control unvaccinated children (11–15). Histological examination of the lungs of the most severely affected children at autopsy revealed peribronchiolar infiltration and increased levels of eosinophils in the lungs and blood (12). This was one of the first demonstrations of immune-mediated injury as the result of vaccination in humans. Thus, before a new vaccine can be developed, a better understanding of the pathogenesis of the RSV vaccine-enhanced illness is critical.

The enhanced pathology exhibited by the children that received the FI-RSV vaccine can be simulated by priming BALB/c mice either with FI-RSV (16–18) or with a recombinant vaccinia virus (vv) expressing the G glycoprotein of RSV (vvG) (19) followed by intranasal inoculation with infectious RSV. In this latter model the vvG-primed mice develop pulmonary eosinophilia following intranasal RSV infection (19). This influx of eosinophils into the lung resembles the pathology found in the children from the 1960's vaccine trials discussed above. Studies using the BALB/c model have suggested that the induction of memory CD4$^+$ T cells producing Th2 cytokines as the result of vvG vaccination mediates enhanced disease (19–21). Transfer of RSV G-specific Th2 CD4$^+$ T cell lines into naive recipients has been shown to induce lung eosinophilia following intranasal RSV infection (20). In addition, analysis of several RSV G protein frameshift mutants has revealed that a particular region spanning aa 193–205 of the G protein is required to induce pulmonary eosinophilia, a process that is dependent on CD4$^+$ T cell recognition of G (22). Furthermore, a separate study established that immunization of BALB/c mice with a peptide derived from aa 184–198 of the G protein led to the development of pulmonary eosinophilia after intranasal infection with RSV (23). Finally, recent studies from our laboratory have demonstrated that both Th1 and Th2 CD4$^+$ T cells are elicited to a single RSV G-derived peptide encompassing aa 183–197 (24). Since lung and blood eosinophilia were also seen in human FI-RSV vaccinees with augmented disease, it is likely that lung pathology induced by FI-RSV or vvG immunization results from priming of Th2

*Beirne B. Carter Center for Immunology Research and †Departments of Microbiology and Pathology, University of Virginia Health Sciences Center, Charlottesville, VA 22908

Received for publication June 26, 2000. Accepted for publication September 6, 2000.

The costs of publication of this article were defrayed in part by the payment of page charges. This article must therefore be hereby marked *advertisement* in accordance with 18 U.S.C. Section 1734 solely to indicate this fact.

[1] This work was supported by U.S. Public Health Service Training Grant AI07496 (to S.M.V. and E.L.W.) and Research Grants AI34607 and AI37293 (to T.J.B.).

[2] Address correspondence and reprint requests to Dr. Thomas J. Braciale, Beirne B. Carter Center for Immunology Research, MR-4 Building, 400 Lane Road, Room 4012, University of Virginia, Charlottesville, VA 22908. E-mail address: tjb2r@virginia.edu

[3] Abbreviations used in this paper: RSV, respiratory syncytial virus; FI, formalin-inactivated; vv, vaccinia virus; vvG, vv expressing the G glycoprotein of RSV; vvB-gal, recombinant vv expressing β-galactosidase; p.i., postinfection; HEL, hen egg lysozyme.

0022-1767/00/$02.00

memory $CD4^+$ T cells. Thus, these observations implicate RSV G-specific memory $CD4^+$ T cells as likely mediators of the immunopathology observed in FI-RSV-vaccinated individuals following natural RSV infection.

Despite the importance of RSV G-specific memory $CD4^+$ T cells in mediating experimental RSV vaccine-enhanced disease, very little quantitative information currently exists concerning this population at the site of RSV infection, the lung. In addition, the fine specificity of the RSV G-specific memory $CD4^+$ T cell population is presently undefined. To address both of these important issues, we sought to better characterize the RSV G protein-specific memory $CD4^+$ T cell response in terms of both its magnitude and its fine specificity. Intracellular cytokine analysis of lung-derived memory effector $CD4^+$ T cells from vvG-sensitized mice infected with RSV revealed that >40% of the $CD4^+$ T cells produced IFN-γ or TNF-α following stimulation with a peptide spanning the immunodominant region of the G protein of RSV. Using a series of analogue peptides truncated at either the amino- or carboxyl-terminal end of the immunodominant region of RSV $G_{183–197}$, we demonstrate that there is a single I-E^d-restricted $CD4^+$ T cell epitope with a core 9-aa sequence of 185–193 that is recognized by both Th1 and Th2 memory effector $CD4^+$ T cells. Strikingly, we also report that the RSV G-specific memory effector $CD4^+$ T cells that have entered the lung following pulmonary RSV infection predominantly express Vβ14 TCR. These results demonstrate for the first time that RSV G-specific effector $CD4^+$ T cells are directed to a single immunodominant I-E^d-restricted G epitope and employ TCR with a highly conserved TCR Vβ-chain.

Materials and Methods

Mice

Female BALB/cAnNTac (H-2^d) mice were purchased from Taconic Farms (Germantown, NY) and used at 8–12 wk of age for all experiments. Mice were housed in a pathogen-free environment.

Viruses and infection of mice

Recombinant vv expressing the attachment (vvG) glycoprotein of RSV was a gift from J. L. Beeler (Food and Drug Administration, National Institutes of Health, Bethesda, MD). The generation and characterization of this virus have been described previously (25). Recombinant vv expressing β-galactosidase (vvB-gal) was used as a negative control. The A2 strain of RSV was a gift from P. L. Collins (National Institute of Allergy and Infectious Diseases, National Institutes of Health). RSV was grown in HEp-2 cells (American Type Culture Collection, Manassas, VA). Groups of four mice were infected with 3×10^6 PFU of vvG or vvB-gal in a 10-μl volume by scarification with a 25-gauge needle at the base of the tail. Three weeks after priming, mice were lightly anesthetized with metaphane (Malinckrodt Veterinary, Mundelein, IL) and intranasally inoculated with 2×10^6 PFU of RSV in 50 μl. At various times postinfection (p.i.), control and infected mice were sacrificed by cervical dislocation.

Peptides

The following peptides were used: hen egg lysozyme $(HEL)_{108–119}$ (WVAWRNRCKGTD) (26) and mouse hepatitis virus N 267–275 (ILNK PRQKR) (27) in addition to the RSV G protein-derived peptides shown in Tables II and III. All peptides were synthesized by the University of Virginia Biomolecular Research Facility using standard techniques of F-moc chemistry.

Preparation of lung-derived lymphocytes

The lung vascular bed was flushed via the right ventricle with 4–5 ml of PBS containing 10 U/ml heparin (Sigma, St. Louis, MO) to remove any blood. The lungs were removed aseptically; carefully dissected away from the heart, the thymus, and the bronchial lymph nodes; and placed into RPMI medium (Life Technologies Laboratories, Grand Island, NY) supplemented with 10% FCS (Atlanta Biologicals, Norcross, GA), 10 U/ml penicillin G, 10 μg/ml streptomycin sulfate, 2 mM L-glutamine, 5×10^{-5} 2-ME, 1 mM sodium pyruvate (Life Technologies), 0.1 mM nonessential amino acids (Life Technologies), and 10 mM HEPES (Life Technologies). The tissue was finely minced and pressed through a wire screen. Particulate matter was removed by quick centrifugation at 1000 rpm. Lung mononuclear cells were obtained by preparing single-cell suspensions from a pool of four mice per group. Cells were counted and resuspended at the given cell concentrations for the appropriate in vitro assay.

Flow cytometric analysis and intracellular cytokine staining

For multicolor FACS analysis, approximately 2×10^6 cells were stained with PE-conjugated anti-CD4 (clone RM4-5) and one of the following FITC-conjugated mAb: anti-LFA-1 (clone 2D7), anti-CD25 (clone 7D4), anti-CD44 (clone IM7), anti-CD62L (clone MEL-14), anti-CD69 (clone H1.2F3), rat IgM (clone R4-22), rat IgG2a (clone R35-95), rat IgG2b (clone A95-1), or hamster IgG (clone A19-3) in PBS supplemented with 2% FCS and 0.02% NaN_3 (staining buffer). All mAb used in FACS staining were purchased from PharMingen (San Diego, CA). Stained cells were fixed and E lysed with FACS lysing solution (Becton Dickinson, San Jose, CA) washed, resuspended in staining buffer, and analyzed in two-color mode using a Becton Dickinson FACScalibur flow cytometer (Mountain View, CA).

For intracellular cytokine staining approximately 2×10^6 cells were stimulated for 5 h in the presence of 1 μg/ml of brefeldin A (Sigma) in the presence (1 μM) or the absence of one of the RSV G protein-derived peptides (or control I-E^d-restricted peptide derived from HEL and/or mouse hepatitis virus). In some experiments, an anti-I-A^d (clone 34-5-3) or anti-I-A^d/I-E^d (clone M5/114.15.2) mAb was added to the culture for the duration of the stimulation. The cells were subsequently washed in staining buffer, blocked with purified anti-FcγRII/III mAb (clone 2.4G2; PharMingen), and stained with CD4-allophycocyanin. After fixation with FACS lysing solution, the cells were washed in permeabilization buffer (staining buffer containing 0.5% saponin; Sigma) and stained with PE-conjugated anti-cytokine mAb or an isotype-matched control mAb (all from PharMingen). The following mAb were used: anti-IL-2 (clone JES6-5H4), anti-IL-3 (clone MP2-8F8), anti-IL-4, (clone BVD4-1D11), anti-IL-5 (clone TRFK5), anti-IL-6 (clone MP5-20F3), anti-IL-10 (clone JES5-16E3), anti-GM-CSF (clone MP1-22E9), anti-IFN-γ (clone XMG1.2), anti-TNF-α, rat IgG1 (clone R3-34), rat IgG2a (clone R35-95), and rat IgG2b (clone A95-1). Control cells known to express the cytokine of interest were used in all experiments as positive controls (MiCK-1, MiCK-2, and MiCK-3; PharMingen). Background staining with the appropriate isotype-matched control mAb was subtracted from each individual. Single-color controls were used in all multiparameter FACS analyses for electronic compensation, and between 60,000 and 80,000 events were acquired from each preparation. Lymphocyte populations were first gated based on forward scatter and 90° side scatter and then analyzed using CellQuest software (Becton Dickinson).

Restimulation in vitro and cytokine ELISA

Cultures of 2×10^6 lung mononuclear cells pooled from four mice per group were incubated in the presence or the absence of one of the RSV G-derived peptides and incubated at 37°C in 1-ml total volume of RPMI-10% FCS supplemented as described above in 24-well plates (Costar, Cambridge, MA). Supernatants were harvested at 24, 48, and 72 h and stored at −80°C before being assayed for cytokines by ELISA according to the manufacturer's instructions. Briefly, Immulon 2 plates (Dynatech, Chantilly, VA) were coated overnight at 4°C with anti-cytokine mAb, washed the next day with PBS-0.05% Tween-20 (Sigma), and blocked with PBS-10% FCS. Samples were added at 50 μl/well, and a standard curve was constructed for each plate by using eight 2-fold dilutions of recombinant cytokine. Following the addition of the samples, the plates were incubated overnight at 4°C before the addition of biotinylated anti-cytokine mAb. Avidin-peroxidase (Sigma) followed by the peroxidase substrate, 3,3′,5,5′-tetramethyl-benzidine dihydrochloride (Sigma) were used to develop the ELISA. The reaction was stopped with 2 N H_2SO_4. Plates were read at 450 nm using an EL 340 plate reader and analyzed using DeltaSoft 3 software (both from Bio-Tek Instruments, Winooski, VT). The following pairs of mAb were used: anti-IL-2, JES6-1A12 and biotinylated JES6-5H4; anti-IL-4, 11B11 and biotinylated BVD6-24G2; anti-IL-5, TRFK5 and biotinylated TRFK4; anti-IL-6, MP5-20F3 and biotinylated MP5-32C11; anti-IL-10, JES5-2A5 and biotinylated SXC-1; anti-IFN-γ, R4-6A2 and biotinylated XMG1.2 (all from PharMingen). Purified and biotinylated anti-IL-13 mAb were purchased from R&D Systems (Minneapolis, MN). Recombinant murine IL-2, IL-4, IL-5, IL-6, IL-10, IFN-γ (PharMingen), and IL-13 (R&D Systems) were used as standards. The limit of detection was

31 pg/ml for IL-2, 125 pg/ml for IL-4, 63 pg/ml for IL-5, 63 pg/ml for IL-6, 156 pg/ml for IL-10, 125 pg/ml for IL-13, and 312 pg/ml for IFN-γ.

Enzyme-linked immunospot assays

Nitrocellulose-based 96-well microtiter plates (Millititer HA, Millipore, Bedford, MA) were coated overnight at 4°C with 5 μg/ml of either anti-IL-5 (clone TRFK5, PharMingen) or anti-IFN-γ (clone R4-6A2, PharMingen) mAb diluted in PBS, washed the next day with PBS, and blocked with RPMI-10% FCS. After washing with PBS, lung mononuclear cells pooled from four mice per group were added to the wells (1×10^5 to 7.8×10^2 cells/well as responders with 2×10^6 peptide-pulsed irradiated (2000 rad) splenocytes as stimulators) in RPMI 1640–10% FCS in a total volume of 200 μl/well. Following the addition of the samples, the plates were incubated overnight at 37°C for 48 h, washed with PBS-0.05% Tween-20 (Sigma) before the addition of biotinylated anti-cytokine mAb (anti-IL-5 clone TRFK4 and anti-IFN-γ clone XMG1.2, both from PharMingen), followed by avidin-peroxidase (1/400 dilution; Sigma). Spots were visualized by developing with the substrate 3-amino-9-ethylcarbazole (Sigma). All assays were performed in triplicate, and mean number of cytokine-secreting cells was calculated from the triplicate assays.

Results

Phenotype and quantitation of the lung-derived CD4$^+$ T cells following RSV infection of vvG-primed BALB/c mice

Examination of activation marker expression on CD4$^+$ T cells infiltrating the lungs of vvG-primed mice challenged with RSV revealed that most of the CD4$^+$ T cells in the lungs express a LFA-1^{high}CD44^{high}CD62L^{low} activated phenotype by days 5–6 p.i. (Fig. 1). Expression of the early activation markers CD25 and CD69 peaked earlier on days 3–4 p.i. In contrast, mice that had been vvG-primed but not infected with RSV did not have CD4$^+$ T cells expressing a highly activated phenotype. Moreover, CD4$^+$ T cells from control mice (i.e., primed with vvB-gal) undergoing a primary RSV infection exhibited a slightly delayed development of the activated phenotype on day 5 p.i. compared with the accelerated memory response that occurred by day 3 p.i. in vvG-primed mice. Thus, as expected, the majority of the CD4$^+$ T cells accumulating in the lungs of vvG-primed mice in response to RSV infection express an activated/memory cell phenotype.

We have recently shown that CD4$^+$ T cells producing both Th1 and Th2 cytokines are elicited to a single RSV G-derived peptide encompassing aa 183–197 (24). To quantitate the frequency of RSV G peptide-specific CD4$^+$ T cells in vvG-primed mice challenged with RSV, we examined cytokine production at the single-cell level using intracellular cytokine staining of lung mononuclear cells stimulated with the RSV $G_{183–197}$ peptide. Table I demonstrates that a high frequency of cytokine-producing CD4$^+$ T cells are elicited to this single peptide. By day 5 p.i., >40% of the CD4$^+$ T cells made IFN-γ or TNF-α following peptide stimulation. The peak in the percentage of CD4$^+$IFN-γ$^+$ cells was on day 5 p.i. This was also the peak in the total number of CD4$^+$ IFN-γ$^+$ cells in the lung. The mean numbers of total CD4$^+$IFN-γ$^+$ cells from four mice per group were as follows: day 3, 2.1×10^5; day 4, 1.5×10^6; day 5, 7.4×10^6; day 6, 5.1×10^6; day 7, 3.5×10^6; and day 9, 1.9×10^6. We also observed a peak in the percentage of CD4$^+$ T cells capable of producing the cytokines IL-3 and GM-CSF on day 5 p.i. In addition, by day 6 p.i., >20% of the lung CD4$^+$ T cells produced another Th1-associated cytokine, IL-2 following peptide stimulation. We were unable to detect CD4$^+$ T cells secreting the Th2-associated cytokines IL-4 and IL-5 in response to the $G_{183–197}$ peptide by intracellular cytokine staining (data not shown). However, we were able to detect a slight (<1.5%) increase in the percentage of IL-10-producing CD4$^+$ T cells. Interestingly, we did observe a more significant 10–15% increase in the percentage of IL-6-producing CD4$^+$ T cells that was not dependent on peptide stimulation (data not shown). The percentage of cytokine-secreting CD4$^+$ T cells in response to peptide was low (<3%) in vvG-primed mice without a challenge infection with RSV or in mice undergoing a primary RSV infection (vvB-gal-primed, RSV day 5 p.i.). Thus, these results demonstrate that RSV infection of vvG-primed mice results in a substantial influx of memory effector CD4$^+$ T cells into the lung that predominantly express an activated cell phenotype and that as many as 40% are capable of producing the effector cytokines IFN-γ and/or TNF-α following stimulation with the $G_{183–197}$ peptide.

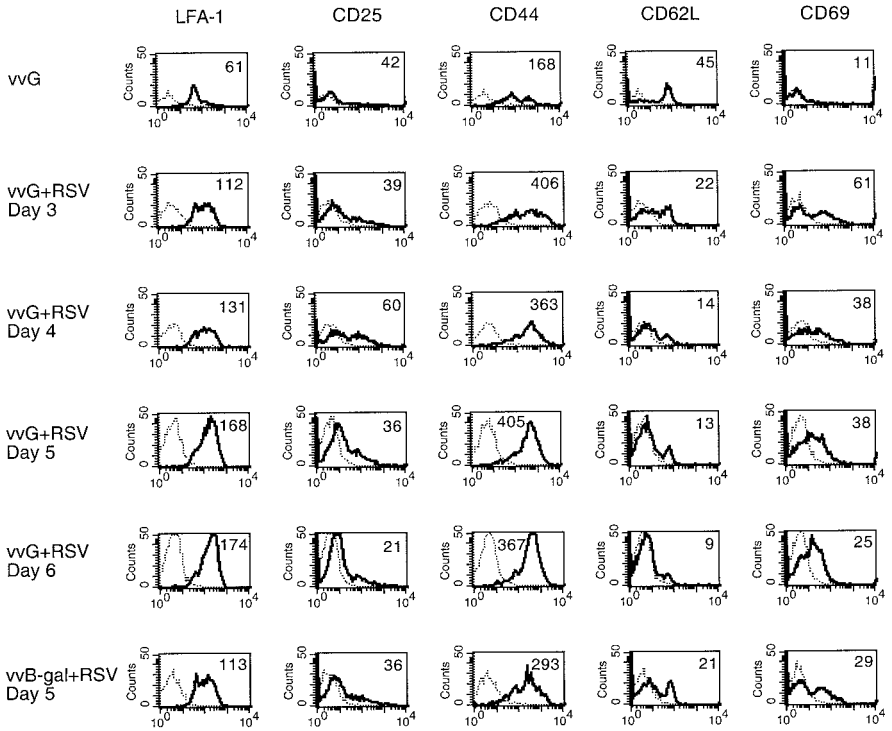

FIGURE 1. Expression of activation markers on lung-derived memory effector CD4$^+$ T cells during RSV infection of vvG-primed mice. Lung cells were stained with anti-CD4 and anti-LFA-1, anti-CD25, anti-CD44, anti-CD62L, or anti-CD69 mAb. A CD4 gate was applied, and the histograms represent the cell surface expression of the indicated mAb on the gated CD4$^+$ T cells. The dotted line represents staining with an isotype-matched control mAb. The number in each histogram represents the mean fluorescence intensity for the indicated mAb. Data shown are representative of two separate experiments with a pool of two mice per experiment.

Table I. *Percentage of lung CD4$^+$ cytokine$^+$ T cells during RSV infection*

Day p.i.	IL-2	IL-3	IFN-γ	TNF-α	GM-CSF
vvG	1.5	0.1	0	0.2	0.1
vvB-gal+RSV Day 5	1.9	0.1	1.3	2.5	0.4
vvG+RSV Day 3	1.2	0.3	4.2	2.6	1.2
vvG+RSV Day 4	6.8	1.7	16.6	13.9	9.3
vvG+RSV Day 5	10.2	2.8	42.4	41.4	23.7
vvG+RSV Day 6	21.3	1.3	39.3	43.1	15.7
vvG+RSV Day 7	18.5	0.8	34.9	32.4	9.9
vvG+RSV Day 9	9.3	0.3	25.4	29.5	4.0

Table II. *Sequences of RSV G protein-derived peptides used in this study*

Peptide	Sequence
RSV 183–197	WAICKRIPNKKPGKK
RSV 183–195	WAICKRIPNKKPG
RSV 183–193	WAICKRIPNKK
RSV 183–192	WAICKRIPNK
RSV 184–193	AICKRIPNKK
RSV 184–192	AICKRIPNK
RSV 184–197	AICKRIPNKKPGKK
RSV 185–197	ICKRIPNKKPGKK
RSV 186–197	CKRIPNKKPGKK
RSV 187–197	KRIPNKKPGKK

Identification of the minimal core sequence recognized by RSV G peptide-specific memory effector CD4$^+$ T cells

The above experiments demonstrate the presence of memory effector CD4$^+$ T cells at a high frequency in the lungs of vvG-primed mice after intranasal RSV challenge using intracellular cytokine staining to detect IFN-γ production following stimulation with a peptide representing aa 183–197 of the G glycoprotein of RSV. Therefore, we chose to use this sensitive single-cell assay to more finely map the CD4$^+$ T cell epitope(s) contained within the 183–197 region of RSV G. To verify that we were using an optimal peptide concentration to stimulate cytokine production by lung-derived effector CD4$^+$ T cells in the intracellular IFN-γ assay, we performed a peptide dose-response curve using the RSV $G_{183–197}$ peptide. Fig. 2 shows that the maximal percentage of IFN-γ-producing CD4$^+$ T cells is elicited at a peptide concentration of 1 μM and higher. In contrast, no increase in the percentage of IFN-γ-producing CD4$^+$ T cells was observed following stimulation with a control I-E^d binding peptide derived from HEL.

The 183–197 peptide contains three overlapping sequences that fit the I-E^d peptide motif (28). To more clearly define the CD4$^+$ T cell epitope(s) within this region, a series of truncated synthetic peptides of different lengths spanning aa 183–197 were synthesized (Table II), and tested for their capacity to stimulate the production of IFN-γ by lung-derived memory effector CD4$^+$ T cells from vvG-primed mice 5 days after intranasal challenge infection with RSV. Fig. 3 demonstrates that peptides with successive aa deletions from the N-terminus are stimulatory until the isoleucine at aa position 185 is deleted. Consecutive deletions from the C-terminus revealed that loss of the lysine at position 193 ablated the ability to stimulate IFN-γ production by these memory effector CD4$^+$ T cells. Fig. 3 also demonstrates that T cell responsiveness was not critically dependent on peptide length, since both the non-stimulatory peptide 183–192 and the stimulatory 184–193 peptide are 10 aa residues in length. These results suggest that there is a single CD4$^+$ T cell epitope within RSV G requiring a minimal 9-aa core sequence spanning residues 185–193 (see underlined amino acids in Table II). Furthermore, to obtain a significant response, at least two additional amino acids at the N- and C-termini of the core 9 aa sequence are needed (Fig. 3, see peptide 183–195). However, since we could not detect Th2 cytokine production using the intracellular cytokine stain following peptide stimulation of lung effector CD4$^+$ T cells ex vivo, we used the enzyme-linked immunospot assay to determine the relative frequency of IFN-γ- and IL-5-secreting cells specific to the RSV $G_{183–195}$ peptide. The

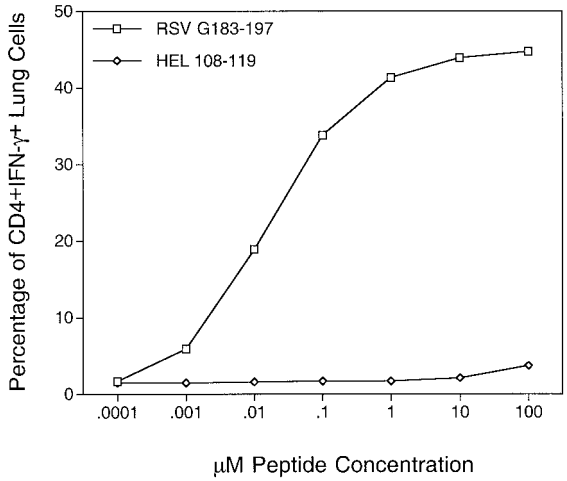

FIGURE 2. Dose response of lung-derived memory effector CD4$^+$ T cells to the RSV $G_{183–197}$ peptide. Lung mononuclear cells from a pool of four vvG-primed mice 5 days after RSV infection were stimulated with the given doses of either a control peptide ($HEL_{108–119}$) or RSV $G_{183–197}$ in the presence of brefeldin A for 5 h and stained for intracellular IFN-γ as described in *Materials and Methods*. One representative of three separate experiments is shown.

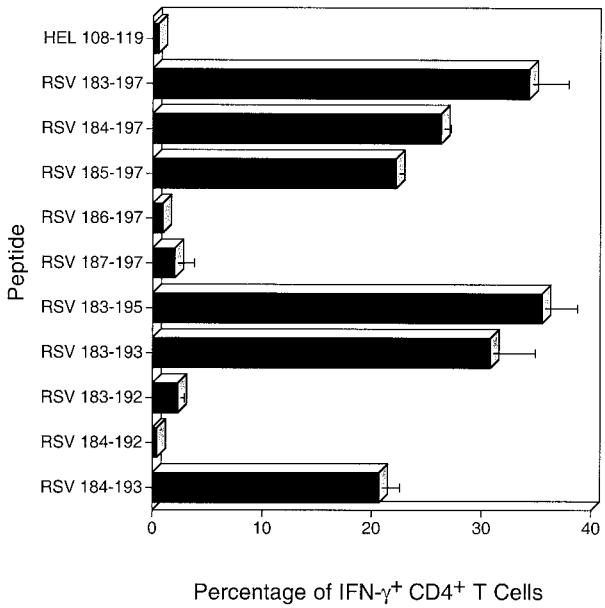

FIGURE 3. Identification of the N- and C-terminal ends of the CD4$^+$ T cell epitope contained within RSV $G_{183–197}$. Lung mononuclear cells from a pool of four vvG-primed mice 5 days after RSV infection were stimulated with 1 μM of the indicated G protein-derived peptide in the presence of Brefeldin A for 5 h and stained for intracellular IFN-γ as described in *Materials and Methods*. The means ± SD from three separate experiments with a pool of four mice per experiment are shown (n = 12/group).

mean numbers of cytokine-secreting cells per million lung mononuclear cells from a representative experiment with a pool of four mice per group were as follows: IFN-γ, 9280; and IL-5, 590. This suggests that there is approximately a 15-fold higher frequency of cells capable of making IFN-γ than IL-5 in response to the RSV $G_{183–195}$ peptide.

To verify that Th2 cytokine production by $CD4^+$ T cells was also dependent on the same core sequence defined above using the intracellular IFN-γ assay, cell culture supernatants of peptide-stimulated lung mononuclear cells isolated 5 days after intranasal RSV challenge of vvG-primed mice were assayed for cytokines by ELISA. As Fig. 4 demonstrates, using the same series of truncated peptides as that used in the intracellular cytokine assay discussed above, that production of the Th1-associated cytokine IFN-γ maps to the same 9-aa core epitope defined by aa 185–193. Moreover, production of the Th2-associated cytokines IL-5 and IL-6 also maps to peptides containing this same core sequence (Fig. 4). Interestingly, another Th2 cytokine, IL-13, appears to map to this same epitope, but in vitro production of IL-13 was more dependent on peptide length. Similar results were obtained with IL-2 and IL-10 as well (data not shown). No IL-4 production was detected following short term stimulation of lung effector T cells on day 5 post-RSV infection (data not shown). Taken together, these results demonstrate that both Th1 and Th2 RSV-specific memory effector $CD4^+$ T cells recognize a single immunodominant epitope in the G protein of RSV with a 9-aa core sequence of 185–193. To insure that the single epitope defined above was indeed restricted to $I\text{-}E^d$, we incubated $CD4^+$ T cells with the 183–197 peptide in the presence of mAb specific either for $I\text{-}A^d$ or for both $I\text{-}A^d/I\text{-}E^d$. Fig. 5 shows that IFN-γ production by $CD4^+$ T cells is inhibited by mAb that recognize both $I\text{-}A^d$ and $I\text{-}E^d$, but not $I\text{-}A^d$ alone, demonstrating that $I\text{-}E^d$ is the restricting MHC molecule for memory effector $CD4^+$ T cells responding to the G epitope containing the 185–193 aa core sequence.

Alanine scan of the RSV $G_{183–195}$ epitope

The above results suggest that there is a single $I\text{-}E^d$-restricted $CD4^+$ T cell epitope within RSV $G_{183–197}$ with a 9-aa core sequence of 185–193. To further analyze the specificity of the RSV-specific memory effector $CD4^+$ T cells, 12 variant peptides were synthesized in which individual residues within the optimal 183–195 sequence (see Fig. 3) were replaced by alanine to determine the amino acids critical for T cell stimulation (Table III). These alanine-substituted peptides were used to stimulate IFN-γ production by RSV G-specific memory effector lung $CD4^+$ T cells using the intracellular IFN-γ assay. Fig. 6 shows that the substitution of alanine for isoleucine at position 185 or arginine at position 188 greatly abolished T cell recognition and IFN-γ production, consistent with the predicted roles of these two aa as $I\text{-}E^d$ anchor residues. Alanine substitution at the two other predicted $I\text{-}E^d$ anchor residues (i.e., aa 190 and 193) also results in significant inhibition of IFN-γ production. However, of particular note was the finding that alanine substitution at position 187, 189, 191, or 192 dramatically diminished T cell recognition and IFN-γ production. This result was striking, since these residues probably represent TCR contact residues. While substitution at one of several different TCR contact residues might be expected to affect the recognition of a single $CD4^+$ T cell clone and its progeny, a heterogeneous population of effector $CD4^+$ T cells derived from different clones would be expected to employ a diverse array of TCR with differing sensitivities to substitution at TCR contact residues and therefore might not be expected to be similarly affected by substitution in individual TCR contact residues. For this reason it is noteworthy that substitution at positions outside the minimal core sequence (i.e., position 183, 194, or 195) did not significantly alter recognition by the memory effector $CD4^+$ T cells, although in some instances the composition of a residue flanking the core epitope has been reported to affect $CD4^+$ T cell recognition (29–31). Similar results were observed using ELISA of cell culture supernatants for the Th2 cytokines IL-5, IL-6, IL-10, and IL-13 following in vitro stimulation with the same panel of alanine-substituted peptides (data not shown).

TCR Vβ repertoire of RSV G peptide-specific memory effector $CD4^+$ T cells

Although residues 187, 189, 191, and 192 could represent secondary MHC anchors contributing to the stability of the peptide/MHC complex, the finding that a high proportion of the memory effector

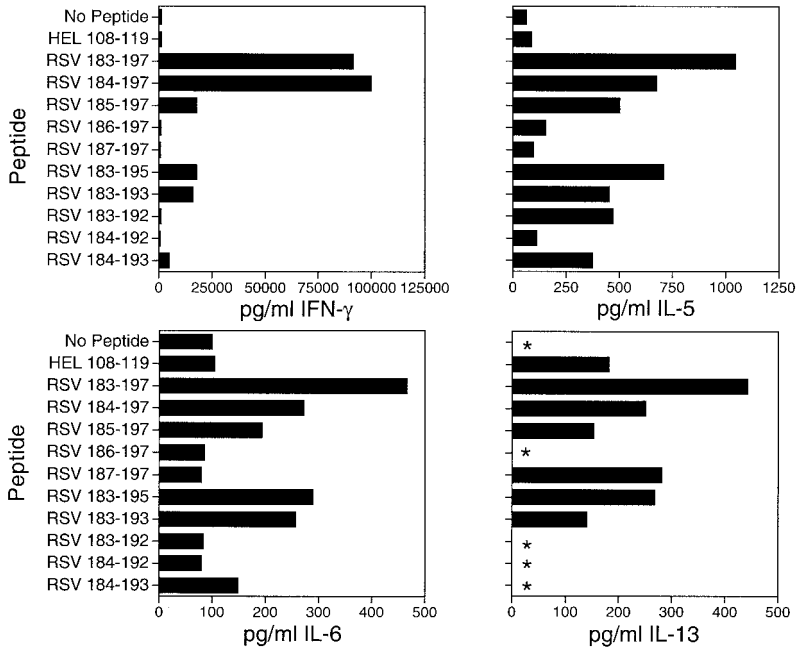

FIGURE 4. Memory effector $CD4^+$ T cells secreting Th2 cytokines also recognize the RSV $G_{185–193}$ epitope. Cultures of lung mononuclear cells from a pool of four vvG-primed mice 5 days after RSV infection were stimulated with 1 μM of the indicated G protein-derived peptide as described in *Materials and Methods*, and culture supernatants were removed at the various times indicated and assessed for cytokine production by ELISA. One representative of three separate experiments is shown.

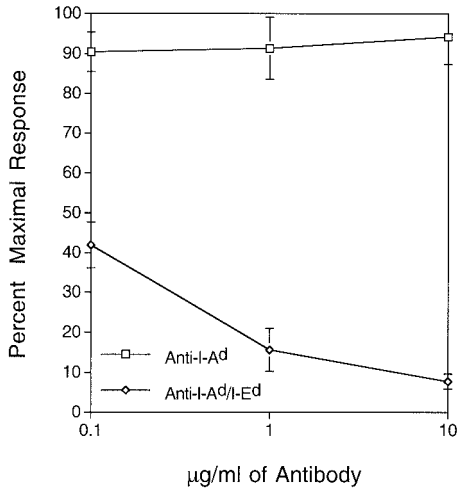

FIGURE 5. The CD4$^+$ T cell epitope in RSV G is I-E^d restricted. Lung mononuclear cells from a pool of four vvG-primed mice 5 days after RSV infection were stimulated with 1 μM RSV $G_{183–197}$ peptide in the presence of brefeldin A for 5 h and stained for intracellular IFN-γ as described in *Materials and Methods*. The means ± SD from three separate experiments with a pool of four mice per experiment are shown (n = 12/group).

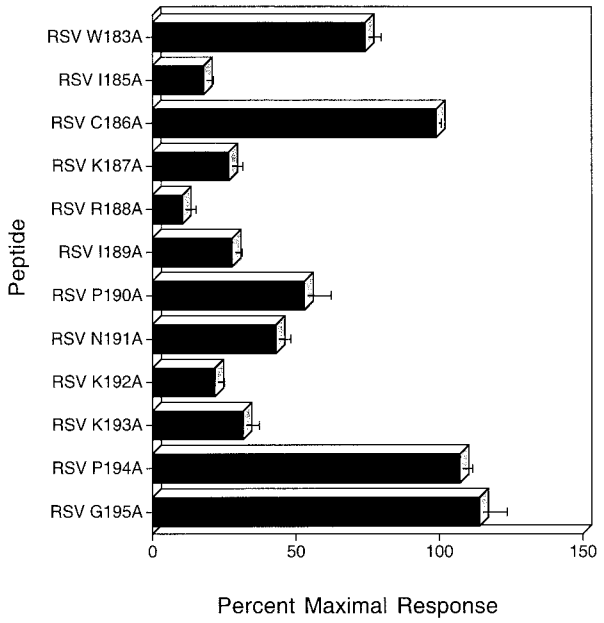

FIGURE 6. Identification of critical residues for T cell recognition of the RSV $G_{183–195}$ region. Lung mononuclear cells from a pool of four vvG-primed mice 5 days after RSV infection were stimulated with 1 μM of the indicated peptide in the presence of brefeldin A for 5 h and stained for intracellular IFN-γ as described in *Materials and Methods*. The means ± SD from three separate experiments with a pool of four mice per experiment are shown (n = 12/group).

CD4$^+$ T cells was equally sensitive to alanine substitutions at $G_{185–193}$ core residues other than the four predicted I-E^d anchor sites suggested that these substitutions may be disrupting potential TCR contact residues necessary for the response of an oligoclonal T cell population. To examine this possibility, we challenged vvG-primed mice with RSV and stained lung-derived effector CD4$^+$ T cells following stimulation with the RSV $G_{183–197}$ peptide for intracellular IFN-γ and TCR Vβ usage using a panel of Vβ-specific mAb. The TCR Vβ repertoires of the IFN-γ^+ and IFN-γ^- CD4$^+$ T cell populations are shown in Fig. 7. Surprisingly, among the activated CD4$^+$ T cells infiltrating the lungs of vvG-primed, RSV-infected mice, both the IFN-γ^+ and IFN-γ^- subsets of CD4$^+$ T cells are highly enriched for Vβ14$^+$ cells. Since we have demonstrated above that both Th1 and Th2 effector CD4$^+$ T cells are elicited to the same I-E^d-restricted epitope, it is likely that the IFN-γ^-Vβ14$^+$ population reflects Th2 CD4$^+$ T cells that we are unable to detect in the intracellular cytokine assay. Thus, RSV infection of vvG-primed BALB/c mice results in the generation and recruitment of a RSV-specific CD4$^+$ T cell population that predominantly expresses a Vβ14 TCR.

Discussion

The BALB/c mouse model of RSV infection has proven to be a valuable tool in dissecting the mechanisms of vaccine-enhanced disease. Although it has been known for some time that CD4$^+$ T cells directed against the RSV G protein may play an important role in mediating vaccine-enhanced immunopathology (32, 33), the specificity and character of the G protein-specific CD4$^+$ T cell response in lungs have remained poorly defined. In this report we set out to examine in detail the effector CD4$^+$ T cell response to the G protein of RSV, and as a result of our analyses we made three important observations. First, RSV infection of vvG-primed mice results in a high frequency of MHC class II-restricted virus-specific memory effector CD4$^+$ T cells that enter the site of infection, the lung. These G-specific memory effector CD4$^+$ T cells are directed to a single I-E^d-restricted immunodominant epitope with a 9-aa core sequence at $G_{185–193}$.

Second, both Th1 and Th2 memory effector CD4$^+$ T cells are directed against the same immunodominant RSV G epitope. Third, the RSV G-specific memory effector CD4$^+$ T cells express a highly restricted Vβ TCR repertoire.

The study of virus-specific T cell populations has been greatly aided by recent technological advances, including the development of tetrameric complexes of MHC glycoprotein loaded with peptides and the staining for intracellular cytokines in cells stimulated with peptides (34, 35), both of which have allowed the direct visualization and quantitation of Ag-specific T cell populations (36). For the most part, these techniques have been used to analyze MHC class I-restricted CD8$^+$ T cells in several different viral and tumor model systems (34, 35, 37–44). These studies have all shown that the magnitude of the Ag-specific CD8$^+$ T cell response is greater than previously recognized. Interestingly, recent results from our laboratory using the influenza model suggest that the use of tetramers to quantitate the frequency of virus-specific CD8$^+$ T cell populations may still result in an underestimate of the total virus-specific CD8$^+$ T cell frequency (45). Nevertheless, the advent of the tetramer technology and the intracellular cytokine stain

Table III. *Sequences of RSV alanine-substituted peptides spanning RSV $G_{183–195}$*

Peptide	Sequence
W 183 A	**A**AICKRIPNKKPG
I 185 A	WA**A**CKRIPNKKPG
C 186 A	WAI**A**KRIPNKKPG
K 187 A	WAIC**A**RIPNKKPG
R 188 A	WAICK**A**IPNKKPG
I 189 A	WAICKR**A**PNKKPG
P 190 A	WAICKRI**A**NKKPG
N 191 A	WAICKRIP**A**KKPG
K 192 A	WAICKRIPN**A**KPG
K 193 A	WAICKRIPNK**A**PG
P 194 A	WAICKRIPNKK**A**G
G 195 A	WAICKRIPNKKP**A**

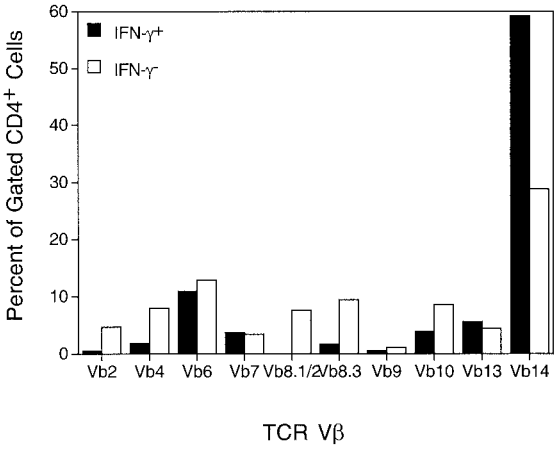

FIGURE 7. TCR repertoire of lung-derived memory effector $CD4^+$ T cells during RSV infection of vvG-primed mice. Lung mononuclear cells from a pool of four vvG-primed mice 5 days after RSV infection were stimulated with 1 μM RSV $G_{183–197}$ peptide in the presence of brefeldin A for 5 h and stained with Abs to CD4, with a panel of TCR Vβ-specific Abs, and with Abs to IFN-γ as described in *Materials and Methods*. A lymphocyte gate was applied, and cells were subsequently gated on either $CD4^+$IFN-γ^+ or $CD4^+$IFN-γ^- cells. The data are the percentage of gated $CD4^+$IFN-γ^+ or $CD4^+$IFN-γ^- cells that express the given Vβ-TCR. One representative of three separate experiments is shown.

have led to a better understanding of the kinetics, phenotype, and frequency of virus-specific $CD8^+$ T cell populations.

In contrast to the great number of studies examining $CD8^+$ T cell responses using these new techniques, much less is known about virus-specific $CD4^+$ T cells. For technical reasons, it is far easier to create stable peptide-loaded MHC class I tetramers than stable MHC class II tetramers. However, in most of the systems studied to date, there is a good correlation between the results obtained with tetramers and intracellular IFN-γ staining (35, 36). Thus, the intracellular cytokine assay probably provides a viable alternative for quantitating virus-specific $CD4^+$ T cell responses. As was the case with virus-specific $CD8^+$ T cells (35, 46), recent work performed in the lymphocytic choriomeningitis virus system has demonstrated that the virus-specific $CD4^+$ T cell frequency is much greater than previously thought (47). In the murine RSV model, there is little information on the frequency of cytokine-secreting virus-specific $CD4^+$ T cells during either an acute RSV infection or a memory response in RSV Ag-primed mice undergoing challenge infection with RSV. One study examined the frequency of MHC class II-restricted CTL by limiting dilution analysis following acute RSV infection, reporting frequencies of $<1\%$ for virus-specific T cells (48). Here we show that by 5 days after RSV infection of vvG-primed BALB/c mice, $>40\%$ of the $CD4^+$ T cells in the lung are specific to a single immunodominant RSV G epitope. This frequency is probably a significant underestimate of the total frequency of RSV G protein-specific $CD4^+$ T cells due to our inability to currently detect peptide-specific $CD4^+$ T cells secreting Th2 cytokines such as IL-4 and IL-5 using the intracellular cytokine assay. Interestingly, others have recently failed to detect IL-4 and/or IL-5 in LCMV peptide-specific $CD4^+$ T cells (49–52). It is currently unclear why no IL-4- or IL-5-secreting $CD4^+$ T cells can be detected using the intracellular cytokine stain, since during murine RSV infection the production of these cytokines can be readily detected in cell culture supernatants following in vitro stimulation with RSV-derived peptides (21) (Fig. 4). It may be that the production of the Th2 cytokines is dependent on the cell cycle status of the $CD4^+$ T cells as has been suggested by several recent studies (53, 54). Future studies comparing the frequency of RSV G peptide-specific $CD4^+$ T cells using the intracellular IFN-γ assay and MHC class II tetramers loaded with the RSV G immunodominant peptide defined in this report should help resolve this important issue.

Crystal structures of peptide/MHC complexes, elution of peptides associated with MHC class II molecules, and peptide binding assays have revealed that MHC anchor residues are usually located at positions 1, 4, 6, and 9 of the core 9 aa that often define $CD4^+$ T cell epitopes (55–60). By analyzing the sequences of peptides known to bind I-E^d molecules, Rammensee et al. were able to define an I-E^d peptide motif with the following preferred aa: W, Y, F, I, L, or V at anchor position 1; K, R, or I at anchor position 4; I, L, V, or G at anchor position 6; and K or R at anchor position 9 (28). Examination of the aa sequence of RSV $G_{183–197}$ revealed three potential $CD4^+$ T cell epitopes (bold indicates the positions of putative I-E^d anchor residues): 184–192 (**A**IC**KR**I**P**N**K**), 185–193 (**I**CK**RI**P NK**K**), and 189–197 (**I**PN**KK**P**P**GK**K**), all of which closely fit the MHC class II I-E^d binding motif. Since these potential epitopes overlap each other, we chose to use the sensitive intracellular cytokine assay to define the N- and C-terminal residues important for recognition of this region by memory effector $CD4^+$ T cells obtained from the lung following a natural RSV infection. Functional screening of a panel of truncated synthetic peptides identified the N- and C-terminal boundaries as aa 185–193, indicating that a single epitope was recognized by RSV G-specific $CD4^+$ T cells capable of secreting Th1 cytokines. We confirmed that Th2 memory effector $CD4^+$ T cells present in the lungs were directed to this single 9-aa core epitope by ELISA analysis of Th2 cytokines secreted into the supernatant of lung memory effector $CD4^+$ T cells stimulated in short term culture with the same series of peptides as that used above in the intracellular IFN-γ assays. To our knowledge, this is the first report using intracellular cytokine staining to define an immunodominant $CD4^+$ T cell epitope recognized by effector $CD4^+$ T cells taken directly from a site of infection. Thus, our results demonstrate the utility of this approach in such epitope-mapping studies.

A series of independent observations by several groups has suggested that there are one or more $CD4^+$ T cell epitopes present in the RSV G glycoprotein located somewhere between residues 183 and 205. Using frameshift mutant G proteins expressed in recombinant vv to sensitize mice, Sparer et al. showed that the region of the G protein between residues 193 and 203 was necessary to induce eosinophilia and weight loss in RSV-infected mice (22). Since eosinophilia is characteristic of a Th2 response (20, 21, 61), these results suggested that a Th2 epitope exists within this region. In contrast, the enhanced weight loss that occurs in vvG-primed mice challenged with RSV is most likely mediated by TNF-α produced by Th1 cells. Thus, the results of Sparer et al. suggest that both a Th1 and a Th2 $CD4^+$ T cell epitope were disrupted by their frameshift mutant analyses. A separate study performed by Tebbey et al. demonstrated that mice primed with a peptide derived from aa 184–198 of RSV G in adjuvant develop eosinophilia following RSV infection (23). More recently, our laboratory has shown that both Th1 and Th2 $CD4^+$ T cells are directed against a single region spanning aa 183–197 of the RSV G glycoprotein (24). Taken together, all these observations pointed to one or more immunodominant $CD4^+$ T cell epitope(s) within aa 183–197 of RSV G. The 9-aa core epitope we have defined here agrees with these previous studies, since this epitope falls within the 184–198 peptide used by Tebbey et al. (23) as well as being within the region of the G protein (i.e., 193–205) disrupted by the studies of Sparer et al. (22). Our results directly demonstrate that a single region of the RSV G protein containing the 185–193 core sequence accounts

for the Th1 and Th2 cytokine response in vvG-primed mice undergoing challenge RSV infection.

In the present study we demonstrate that most of the RSV G peptide-specific $CD4^+$ T cells that can be detected using the intracellular IFN-γ assay express Vβ14 TCR. In addition, we show that approximately 30% of the activated $CD4^+$ T cells that fail to make IFN-γ following peptide stimulation also express Vβ14 TCR. Many of these IFN-γ^- cells may represent virus-specific Th2 $CD4^+$ T cells that are not easily detected using the intracellular cytokine stain. This seems likely, since we have shown here that Th2 cytokines are produced in short term in vitro cultures using the $CD4^+$ epitope we have defined in this report (see Fig. 4). In addition, in vitro activation of lung-derived $CD4^+$ T cells isolated from vvG-primed mice with a Vβ14 TCR-specific mAb induces the production of both Th1 and Th2 cytokines (S. M. Varga and T. J. Braciale, unpublished observations). Thus, it is possible that $CD4^+$ T cells expressing a Vβ14 TCR directed against the immunodominant epitope we have defined in this study may differentiate into either Th1 or Th2 $CD4^+$ T cells in vivo. A previous study examining $CD4^+$ T cells specific to an I-E^d-restricted nucleoprotein epitope of mouse hepatitis virus demonstrated that a single epitope could elicit both Th1 and Th2 $CD4^+$ T cells (27). However, the mouse hepatitis virus nucleoprotein-specific Th1 and Th2 $CD4^+$ T cells expressed TCR with distinctly different Vβ gene usage (27). At present we do not know whether the restricted Vβ usage of the $G_{185–193}$ specific $CD4^+$ T cells reflects the selection of V$\beta14^+$ T cells with a unique TCR β-chain, i.e., a single unique complementarity-determining region 3 or TCR β-chains with limited complementarity-determining region 3 length and sequence diversity. Also, since TCR Vα usage by the memory effector $CD4^+$ T cells has not been analyzed as yet, we cannot determine whether these responding lung effector $CD4^+$ T cells represent a single clone or a panel of memory $CD4^+$ T cell clones with limited TCR diversity. Experiments are in progress to address each of these issues.

A great deal of evidence indicates that MHC class II-restricted $CD4^+$ T cells play an important, yet often unappreciated role in antiviral immunity (2, 62–69). During RSV infection, $CD4^+$ T cells can contribute to the antiviral immune response by providing help for B cells to make antiviral Abs as well as secreting cytokines such as IFN-γ. However, during a RSV memory response, G protein-specific $CD4^+$ T cell responses can also be detrimental to the host by mediating immunopathology and enhancing disease (32, 33, 70). In this report we show that G protein-specific memory $CD4^+$ T cells are directed against a single I-E^d-restricted immunodominant epitope. This epitope elicits a memory response yielding both Th1 and Th2 effector $CD4^+$ T cells. While we cannot formally exclude the possibility that the same effector $CD4^+$ T cell in the lungs is producing both Th1 and Th2 cytokines, our evidence to date supports the view that Th1 and Th2 cytokines are produced by different effector $CD4^+$ T cells. Both these effector cell types may contribute to the enhanced pathology observed in immune individuals. In addition, we have demonstrated for the first time that the majority of RSV G protein-specific $CD4^+$ T cells express a restricted Vβ14 TCR. Such a focused T cell response eliciting both Th1 and Th2 effector cells and capable of mediating enhanced disease could be related to the finding that only a subset of the children who received the FI-RSV vaccine in the 1960s went on to exhibit enhanced disease upon RSV infection (11–15). Our future studies in the murine RSV model will examine whether the $CD4^+$ T cells that exclusively express Vβ14 TCR are capable of mediating RSV vaccine-enhanced disease. Our results suggest that a comparable analysis of $CD4^+$ T cell specificity, effector activity, and TCR usage may be warranted in the human.

Acknowledgments

We thank Julie Burns for secretarial support, and Barbara Small and Sarah Dressel for technical support.

References

1. Biron, C. A. 1994. Cytokines in the generation of immune responses to, and resolution of, virus infection. *Curr. Opin. Immunol. 6:530.*
2. Doherty, P. C., D. J. Topham, R. A. Tripp, R. D. Cardin, J. W. Brooks, and P. G. Stevenson. 1997. Effector $CD4^+$ and $CD8^+$ T-cell mechanisms in the control of respiratory virus infections. *Immunol. Rev. 159:105.*
3. Zinkernagel, R. M. 1996. Immunology taught by viruses. *Science 271:173.*
4. Glezen, W. P., L. H. Taber, A. L. Frank, and J. A. Kasel. 1986. Risk of primary infection and reinfection with respiratory syncytial virus. *Am. J. Dis. Child. 140: 543.*
5. Heilman, C. A. 1990. Respiratory syncytial and parainfluenza viruses. *J. Infect. Dis. 161:402.*
6. Dowell, S. F., L. J. Anderson, H. E. Gary, D. D. Erdman, J. F. Plouffe, T. M. File, B. J. Marston, and R. F. Breiman. 1996. Respiratory syncytial virus is an important cause of community-acquired lower respiratory infection among hospitalized adults. *J. Infect. Dis. 174:456.*
7. Falsey, A. R., J. J. Treanor, R. F. Betts, and E. E. Walsh. 1992. Viral respiratory infections in the institutionalized elderly: clinical and epidemiologic findings. *J. Am. Geriatr. Soc. 40:115.*
8. Falsey, A. R., C. K. Cunningham, W. H. Barker, R. W. Kouides, J. B. Yuen, M. Menegus, L. B. Weiner, C. A. Bonville, and R. F. Betts. 1995. Respiratory syncytial virus and influenza A infections in the hospitalized elderly. *J. Infect. Dis. 172:389.*
9. Harrington, R. D., T. M. Hooton, R. C. Hackman, G. A. Storch, B. Osborne, C. A. Gleaves, A. Benson, and J. D. Meyers. 1992. An outbreak of respiratory syncytial virus in a bone marrow transplant center. *J. Infect. Dis. 165:987.*
10. Mlinaric-Galinovic, G., A. R. Falsey, and E. E. Walsh. 1996. Respiratory syncytial virus infection in the elderly. *Eur. J. Clin. Microbiol. Infect. Dis. 15:777.*
11. Belshe, R. B., L. P. Van Voris, and M. A. Mufson. 1982. Parenteral administration of live respiratory syncytial virus vaccine: results of a field trial. *J. Infect. Dis. 145:311.*
12. Chin, J. C., R. L. Magoffin, L. A. Shearer, J. H. Schieble, and E. H. Lennette. 1969. Field evaluation of a respiratory syncytial virus vaccine and a trivalent parainfluenza virus vaccine in a pediatric population. *Am. J. Epidemiol. 89:449.*
13. Fulginiti, V. A., J. J. Eller, O. F. Sieber, J. W. Joyner, M. Minamitani, and G. Meiklejohn. 1969. Respiratory virus immunization. I. A field trial of two inactivated respiratory virus vaccines; an aqueous trivalent parainfluenza virus vaccine and an alum-precipitated respiratory syncytial virus vaccine. *Am. J. Epidemiol. 89:435.*
14. Kapikian, A. Z., R. H. Mitchell, R. M. Chanock, R. A. Shvedoff, and C. E. Stewart. 1969. An epidemiologic study of altered clinical reactivity to respiratory syncytial (RS) virus infection in children previously vaccinated with an inactivated RS virus vaccine. *Am. J. Epidemiol. 89:405.*
15. Kim, H. W., J. G. Canchola, C. D. Brandt, G. Pyles, R. M. Chanock, K. Jensen, and R. H. Parrott. 1969. Respiratory syncytial virus disease in infants despite prior administration of antigenic inactivated vaccine. *Am. J. Epidemiol. 89:422.*
16. Connors, M., A. B. Kulkarni, C.-Y. Firestone, K. L. Holmes, H. C. Morse, A. V. Sotnikov, and B. R. Murphy. 1992. Pulmonary histopathology induced by respiratory syncytial virus (RSV) challenge of formalin-inactivated RSV-immunized BALB/c mice is abrogated by depletion of $CD4^+$ T cells. *J. Virol. 66:7444.*
17. Tang, Y.-W., and B. S. Graham. 1994. Anti-IL-4 treatment at immunization modulates cytokine expression, reduces illness, and increases cytotoxic T lymphocyte activity in mice challenged with respiratory syncytial virus. *J. Clin. Invest. 94:1953.*
18. Waris, M. E., C. Tsou, D. D. Erdman, S. R. Zaki, and L. J. Anderson. 1996. Respiratory syncytial virus infection in BALB/c mice previously immunized with formalin-inactivated virus induces enhanced pulmonary inflammatory response with a predominant Th2-like cytokine pattern. *J. Virol. 70:2852.*
19. Openshaw, P. J. M., S. L. Clarke, and F. M. Record. 1992. Pulmonary eosinophilic response to respiratory syncytial virus infection in mice sensitized to the major surface glycoprotein G. *Int. Immunol. 4:493.*
20. Alwan, W. H., W. J. Kozlowska, and P. J. M. Openshaw. 1994. Distinct types of lung disease caused by functional subsets of antiviral T cells. *J. Exp. Med. 179:81.*
21. Srikiatkhachorn, A., and T. J. Braciale. 1997. Virus-specific memory and effector T lymphocytes exhibit different cytokine responses to antigens during experimental murine respiratory syncytial virus infection. *J. Virol. 71:678.*
22. Sparer, T., S. Matthews, T. Hussell, A. Rae, B. Garcia-Barreno, J. Melero, and P. Openshaw. 1998. Eliminating a region of respiratory syncytial virus attachment protein allows induction of protective immunity without vaccine-enhanced lung eosinophilia. *J. Exp. Med. 187:1921.*
23. Tebbey, P. W., M. Hagen, and G. E. Hancock. 1998. Atypical pulmonary eosinophilia is mediated by a specific amino acid sequence of the attachment (G) protein of respiratory syncytial virus. *J. Exp. Med. 188:1967.*
24. Srikiatkhachorn, A., W. Chang, and T. J. Braciale. 1999. Induction of Th-1 and Th-2 responses by respiratory syncytial virus attachment glycoprotein is epitope and major histocompatibility complex independent. *J. Virol. 73:6590.*
25. Ball, L. A., K. K. Y. Young, K. Anderson, P. L. Collins, and G. W. Wertz. 1986. Expression of the major glycoprotein G of human respiratory syncytial virus from recombinant vaccinia virus vectors. *Proc. Natl. Acad. Sci. USA 83:246.*
26. Katz, M. E., R. M. Maizels, L. Wicker, A. Miller, and E. E. Sercarz. 1982. Immunological focusing by the mouse major histocompatibility complex: mouse

strains confronted with distantly related lysozymes confine their attention to very few epitopes. *J. Immunol. 12:535.*
27. Van Der Veen, R. C. 1996. Immunogenicity of JHM virus proteins: characterization of a $CD4^+$ T cell epitope on nucleocapsid protein which induces different T-helper cell subsets. *Virology 225:339.*
28. Rammensee, H.-G., T. Friede, and S. Stevanovic. 1995. MHC ligands and peptide motifs: first listing. *Immunogenetics 41:178.*
29. Carson, R. T., K. M. Vignali, D. L. Woodland, and D. A. A. Vignali. 1997. T cell receptor recognition of MHC class II-bound peptide flanking residues enhances immunogenicity and results in altered TCR V region usage. *Immunity 7:387.*
30. Moudgil, K. D., E. E. Sercarz, and I. S. Grewal. 1998. Modulation of the immunogenicity of antigenic determinants by their flanking residues. *Immunol. Today 19:217.*
31. Vignali, D. A. A., and J. L. Strominger. 1994. Amino acid residues that flank core peptide epitopes and the extracellular domains of CD4 modulate differential signaling through the T cell receptor. *J. Exp. Med. 179:1945.*
32. Alwan, W. H., F. M. Record, and P. J. M. Openshaw. 1992. $CD4^+$ T cells clear virus but augment disease in mice infected with respiratory syncytial virus. Comparison with the effects of $CD8^+$ T cells. *Clin. Exp. Immunol. 88:527.*
33. Alwan, W. H., and P. J. M. Openshaw. 1993. Distinct patterns of T- and B-cell immunity to respiratory syncytial virus induced by individual viral proteins. *Vaccine 11:431.*
34. Altman, J. D., P. A. H. Moss, P. J. R. Goulder, D. H. Barouch, M. G. McHeyzer-Williams, J. I. Bell, A. J. McMichael, and M. M. Davis. 1996. Phenotypic analysis of antigen-specific T lymphocytes. *Science 274:94.*
35. Murali-Krishna, K., J. D. Altman, M. Suresh, D. J. D. Sourdive, A. J. Zajac, J. D. Miller, J. Slansky, and R. Ahmed. 1998. Counting antigen-specific CD8 T cells: a reevaluation of bystander activation during viral infection. *Immunity 8:177.*
36. Doherty, P. C., and J. P. Christensen. 2000. Accessing complexity: the dynamics of virus-specific T cell responses. *Annu. Rev. Immunol. 18:561.*
37. Belz, G. T., J. D. Altman, and P. C. Doherty. 1998. Characteristics of virus-specific $CD8^+$ T cells in the liver during the control and resolution phases of influenza pneumonia. *Proc. Natl. Acad. Sci. USA 95:13812.*
38. Bieganowska, K., P. Hollsberg, G. J. Buckle, D.-G. Lim, T. F. Greten, J. Schneck, J. D. Altman, S. Jacobson, S. L. Ledis, B. Hanchard, et al. 1999. Direct analysis of viral-specific $CD8^+$ T cells with soluble HLA-A2/Tax11–19 tetramer complexes in patients with human T cell lymphotropic virus-associated myelopathy. *J. Immunol. 162:1765.*
39. Callan, M. F. C., L. Tan, N. Annels, G. S. Ogg, J. D. K. Wison, C. A. O'Callaghan, N. Steven, A. J. McMichael, and A. B. Rickinson. 1998. Direct visualization of antigen-specific $CD8^+$ T cells during the primary immune response to Epstein-Barr virus in vivo. *J. Exp. Med. 187:1395.*
40. Crawford, F., H. Kozono, J. White, P. Marrack, and J. Kappler. 1998. Detection of antigen-specific T cells with multivalent soluble class II MHC covalent peptide complexes. *Immunity 8:675.*
41. Flynn, K., G. Belz, J. Altman, R. Ahmed, D. Woodland, and P. Doherty. 1998. Virus-specific $CD8^+$ T cells in primary and secondary influenza pneumonia. *Immunity 8:683.*
42. Greten, T. F., J. E. Slansky, R. Kubota, S. S. Soldan, E. M. Jaffee, T. P. Leist, D. M. Pardoll, S. Jacobson, and J. P. Schneck. 1998. Direct visualization of antigen-specific T cells: HTLV-1 Tax11–19-specific $CD8^+$ T cells are activated in peripheral blood and accumulate in cerebrospinal fluid from HAM/TSP patients. *Proc. Natl. Acad. Sci. USA 95:7568.*
43. Kuroda, M. J., J. E. Schmitz, D. H. Barouch, A. Craiu, T. M. Allen, A. Sette, D. I. Watkins, M. A. Forman, and N. L. Letvin. 1998. Analysis of Gag-specific cytotoxic T lymphocytes in simian immunodeficiency virus-infected rhesus monkeys by cell staining with a tetrameric major histocompatibility complex class I-peptide complex. *J. Exp. Med. 187:1373.*
44. Lukacher, A. E., J. M. Moser, A. Hadley, and J. D. Altman. 1999. Visualization of polyoma virus-specific $CD8^+$ T cells in vivo during infection and tumor rejection. *J. Immunol. 163:3369.*
45. Spencer, J. V., and T. J. Braciale. 2000. Incomplete $CD8^+$ T lymphocyte differentiation as a mechanism for subdominant cytotoxic T lymphocyte responses to a viral antigen. *J. Exp. Med. 191:1687.*
46. Butz, E. A., and M. J. Bevan. 1998. Massive expansion of antigen-specific $CD8^+$ T cells during an acute virus infection. *Immunity 8:167.*
47. Varga, S. M., and R. M. Welsh. 1998. Cutting edge: detection of a high frequency of virus-specific $CD4^+$ T cells during acute infection with lymphocytic choriomeningitis virus. *J. Immunol. 161:3215.*
48. Tripp, R. A., and L. J. Anderson. 1998. Cytotoxic T-lymphocyte precursor frequencies in BALB/c mice after acute respiratory syncytial viral (RSV) infection or immunization with a formalin-inactivated RSV vaccine. *J. Virol. 72:8971.*
49. Kamperschroer, C., and D. G. Quinn. 1999. Quantification of epitope-specific MHC class-II-restricted T cells following lymphocytic choriomeningitis virus infection. *Cell. Immunol. 193:134.*
50. Su, H. C., L. P. Cousens, L. D. Fast, M. K. Slifka, R. D. Bungiro, R. Ahmed, and C. A. Biron. 1998. $CD4^+$ and $CD8^+$ T cell interactions in IFN-γ and IL-4 responses to viral infections: requirements for IL-2. *J. Immunol. 160:5007.*
51. Varga, S. M., and R. M. Welsh. 2000. High frequency of virus-specific interleukin-2-producing $CD4^+$ T cells and Th1 dominance during lymphocytic choriomeningitis virus infection. *J. Virol. 74:4429.*
52. Whitmire, J. K., M. S. Asano, K. Murali-Krishna, M. Suresh, and R. Ahmed. 1998. Long-term CD4 Th1 and Th2 memory following acute lymphocytic choriomeningitis virus infection. *J. Virol. 72:8281.*
53. Bird, J. J., D. R. Brown, A. C. Mullen, N. H. Moskowitz, M. A. Mahowald, J. R. Sider, T. F. Gajewski, C.-R. Wang, and S. L. Reiner. 1998. Helper T cell differentiation is controlled by the cell cycle. *Immunity 9:229.*
54. Richter, A., M. Lohning, and A. Radbruch. 1999. Instruction for cytokine expression in T helper lymphocytes in relation to proliferation and cell cycle progression. *J. Exp. Med. 190:1439.*
55. Fremont, D. H., W. A. Hendrickson, P. Marrack, and J. Kappler. 1996. Structures of an MHC class II molecule with covalently bound single peptides. *Science 272:1001.*
56. Fremont, D. H., D. Monnaie, C. A. Nelson, W. A. Hendrickson, and E. R. Unanue. 1998. Crystal structure of $I\text{-}A^k$ in complex with a dominant epitope of lysozyme. *Immunity 8:305.*
57. Jorgensen, J. L., P. A. Reay, E. W. Ehrich, and M. M. Davis. 1992. Molecular components of T-cell recognition. *Annu. Rev. Immunol. 10:835.*
58. Reay, P. A., R. M. Kantor, and M. M. Davis. 1994. Use of global amino acid replacements to define the requirements for MHC binding and T cell recognition of moth cytochrome *c* (93–103). *J. Immunol. 152:3946.*
59. Scott, C. A., P. A. Peterson, L. Teyton, and I. A. Wilson. 1998. Crystal structures of two $I\text{-}A^d$-peptide complexes reveal that high affinity can be achieved without large anchor residues. *Immunity 8:319.*
60. Stern, L. J., J. H. Brown, T. S. Jardetzky, J. C. Gorga, R. G. Urban, J. L. Strominger, and D. C. Wiley. 1994. Crystal structure of the human class II MHC protein HLA-DR1 complexed with an influenza virus peptide. *Nature 368: 215.*
61. Srikiatkhachorn, A., and T. J. Braciale. 1997. Virus-specific $CD8^+$ T lymphocytes downregulate T helper cell type 2 cytokine secretion and pulmonary eosinophilia during experimental murine respiratory syncytial virus infection. *J. Exp. Med. 186:421.*
62. Christensen, J. P., O. Marker, and A. R. Thomsen. 1994. The role of $CD4^+$ T cells in cell-mediated immunity to LCMV studies in MHC class I and class II deficient mice. *Scand. J. Immunol. 40:373.*
63. Doherty, P. C., R. A. Tripp, A.-M. Hamilton-Easton, R. D. Cardin, D. L. Woodland, and M. A. Blackman. 1997. Tuning into immunological dissonance: an experimental model for infectious mononucleosis. *Curr. Opin. Immunol. 9:477.*
64. Manickan, E., and B. T. Rouse. 1995. Roles of different T-cell subsets in control of herpes simplex virus infection determined by using T-cell-deficient mouse models. *J. Virol. 69:8178.*
65. McMichael, A. J., and R. E. Phillips. 1997. Escape of human immunodeficiency virus from immune control. *Annu. Rev. Immunol. 15:271.*
66. Pantaleo, G., C. Graziosi, and A. S. Fauci. 1997. Virologic and immunologic events in primary HIV infection. *Springer Semin. Immunopathol. 18:257.*
67. Perelson, A. S., P. Essunger, and D. D. Ho. 1997. Dynamics of HIV-1 and $CD4^+$ lymphocytes in vivo. *AIDS 11:S17.*
68. Thomson, S. A., S. L. Elliott, M. A. Sherritt, K. W. Sproat, B. E. H. Coupar, A. A. Scalzo, C. A. Forbes, A. M. Ladhams, X. Y. Mo, R. A. Tripp, et al. 1996. Recombinant polyepitope vaccines for the delivery of multiple CD8 cytotoxic T cell epitopes. *J. Immunol. 157:822.*
69. Von Herrath, M. G., and M. B. A. Oldstone. 1997. Interferon-γ is essential for destruction of β cells and development of insulin-dependent diabetes mellitus. *J. Exp. Med.* 185:531.
70. Graham, B. S., L. A. Bunton, P. F. Wright, and D. T. Karzon. 1991. Role of T lymphocyte subsets in the pathogenesis of primary infection and rechallenge with respiratory syncytial virus in mice. *J. Clin. Invest. 88:1026.*